





Evaluating the Effects of a Priori Deep Learning Image Synthesis on Multi-Modal MR-to-CT Image Registration Performance

Nils Frohwitter^{1,3} ^a, Alessa Hering² ^b, Ralf Möller^{1,3} ^c and Mattis Hartwig^{1,4} ^d

¹German Research Center for Artificial Intelligence, 23562 Lübeck, Germany

²Fraunhofer MEVIS, Institute for Digital Medicine, 23562 Lübeck, Germany

³Institute of Information Systems, University of Lübeck, 23562 Lübeck, Germany

⁴singularIT GmbH, 04109 Leipzig, Germany

Keywords: Image-to-Image Translation, Image Synthesis, Image Registration.


Abstract: Radiation therapy often requires a computed tomography (CT) for treatment planning and an additional magnetic resonance (MR) imaging prior to the treatment for adaptation. With two different images from the same scene, multi-modal image registration is needed to align areas of interest in both images. One idea to improve the registration process is to perform an image synthesis that converts one image mode into another mode prior to the registration. In this paper, we address the research needed to perform a thorough evaluation of the synthesis step on overall registration performance using different well-known registration methods of the Advanced Normalization Tools (ANTs) framework. Given abdominal images, we use CycleGAN for synthesis and compare the registration performance to the one without synthesis by using four different well-known registration methods. We show that good image synthesizing results lead to an average improvement in all registration methods, biggest improvement being achieved for the ‘Symmetric Normalization’ method with 8% (measured with Dice-score). The overall best registration method with prior synthesis is ‘Symmetric Normalization and Rigid’. Furthermore, we show that the images with bad synthetic results lead to worse registration, thus suggesting the correlation between synthesizing quality and registration performance.


1 INTRODUCTION


Having accurate registration algorithms for multi-modal images is highly needed in the field of image guided radiation therapy. The imaging in radiation therapy is often done in two steps. In the planning phase, an image based on computed tomography (CT) is created to localise the target area and to calculate a dose distribution. Right before the treatment and/or during the treatment phase, further images based on magnetic resonance imaging (MR) or cone-beam computed tomography (CBCT) are taken (Qi, 2017) to deal with global displacements such as the positioning of the patient as well as local changes such as fill levels of organs or reductions in size of tumor tissue. Multi-modal image registration is needed to align areas of interest in the images taken with dif-


ferent imaging techniques and presumably at different times. Especially MR-CT registration is widely used in radiation therapy because of the high soft-tissue contrast and post-treatment analysis with the MR images (Chandarana et al., 2018).

In the past, several authors have worked on deep learning image synthesis to improve the multi-modal image registration task (Wei et al., 2019; McKenzie et al., 2019; Tanner et al., 2018). The idea is that the registration algorithms can focus on the easier task of mono-modal image registration if one image type (e.g. MR) is transformed into the other type (e.g. CT) before the actual registration takes place. In multi-modal registration, it is generally difficult to identify these correspondences or similarity measures because of the often highly different physical properties (Saiti and Theoharis, 2020). Current work lacks the clear evaluation of registration performance using a standardised dataset and multiple registration algorithms. In this paper, we focus on evaluating the influence of MR-to-CT synthesis on the multi-modal image registration performance. Given the abdom-

^a  <https://orcid.org/0000-0001-8267-281X>

^b  <https://orcid.org/0000-0002-7602-803X>

^c  <https://orcid.org/0000-0002-1174-3323>

^d  <https://orcid.org/0000-0002-1507-7647>

inal MR and CT images from the Learn2Reg2021-challenge (Dalca et al., 2021), we perform image-to-image synthesis via the CycleGAN framework to create synthetic CT images and compare the four different registration methods ‘Rigid’, ‘Symmetric Normalization’, ‘Symmetric Normalization and Rigid’ as well as ‘Symmetric Normalization with Elastic Regularization’ of the ANTs framework with and without the synthetic CT image instead of the MR image. We show that good synthesizing results lead to an average improvement in all registration methods. Furthermore, with synthesis the method ‘Symmetric Normalization’ achieves the biggest improvement compared to the non-synthetic registration and ‘Symmetric Normalization and Rigid’ achieves the overall best registration result.

The remainder of the paper is structured as follows. Section 2 covers the preliminaries on the CycleGAN architecture and the process of image registration in general. Section 3 describes the current state-of-the-art of image synthesis and image registration as well as how our work fits into other researches. Section 4 introduces the used dataset with its preprocessing steps. Section 5 describes the experimental setup consisting of image synthesis and image registration. In Section 6, the results are presented and discussed. Lastly, Section 7 gives a short conclusion of the paper.

2 PRELIMINARIES

In this section, we give a short introduction to the important deep learning architectures used in this paper as well as the overall goal and functionality of image registration.

2.1 Deep Learning Architecture

The term *deep learning* (DL) covers techniques that allow for computational models that consist of multiple layers to learn multiple levels of representations. These layers and their weights are not designed by human engineers but are learned from data given a specific task (LeCun et al., 2015). A Generative Adversarial Network (GAN) is a DL concept consisting of two neural networks: a generator G and a discriminator D (Goodfellow et al., 2014). The generator aims to create synthetic images that are indistinguishable from real data by the discriminator. The discriminator on the other hand, aims to identify real and fake data correctly which leads to the so called adversarial training between generator and discriminator. In the training process, the generator synthesizes fake

data and receives feedback of its synthesizing quality through the evaluation of the discriminator. If the discriminator is able to differentiate the fake image correctly, the generator is penalized, otherwise the discriminator is penalized. If the training between those two neural networks is done in a well balanced way, the generator learns to imitate the distribution of the training data. The learning problem was originally formulated as a minmax-problem

$$\min_G \max_D E_{x \sim p_{real}} [\log(D(x))] + E_{z \sim p_z} [\log(1 - D(G(z)))], \quad (1)$$

where p_{real} is the distribution of the training data and p_z of the input noise (Goodfellow et al., 2014).

A problem that arises with GANs is its training instability which can lead to a mode collapse. The discriminator alone cannot assure that the generator creates synthetic data which is either diverse or clearly shows correspondences with the input data. Especially in image-to-image synthesis, it would be problematic if the generator just learns the mapping onto a single image to satisfy the discriminator. To solve the mode-collapse problem in data synthesis, the CycleGAN architecture was developed (Zhu et al., 2017). The CycleGAN consists of two generators and discriminators for synthesizing from both domains onto one another in a cycle consistent way. By using a second generator to synthesize back into the original domain, the recreated image can be compared pixelwise with the original image. For the sake of completeness, DualGAN (Yi et al., 2017) is a related architecture to CycleGAN that has been developed in parallel and has been used to solve similar issues. In this paper, we focus on the CycleGAN architecture.

2.2 Image Registration

Image registration is a mathematical process that involves the determination of a reasonable transformation between one or many target images and one reference image. Image registration is often used to combine information of different image modalities like the high soft-tissue contrast of the MR and the high bone contrast of the CT or to handle images of the same scene taken in different times (Qi, 2017). For more details on medical image registration, see the work of J. Modersitzki (Modersitzki, 2009).

In this paper, we use implemented registration methods from the Advanced Normalization Tools (ANTs) (Avants et al., 2011), more precisely from the python version ANTsPy¹². We choose the transform

¹<https://antspy.readthedocs.io/en/latest/index.html>

²<https://pypi.org/project/antspyx/0.3.3/>

types ‘Rigid’, ‘Symmetric Normalization’ (SyN), ‘Symmetric Normalization and Rigid’ (SyNRA) and ‘Symmetric Normalization with Elastic Regularization’ (ElasticSyN) for registration. To avoid confusion for the reader, we use ‘SyN’ as an abbreviation for ‘Symmetric Normalization’ and ‘syn’ for ‘synthetic’. Rigid transformation only consists of rotation and translation but SyN (Avants et al., 2011) is used as a symmetric diffeomorphic registration method with mutual information as optimization metric, combined with affine transformation as for the ANTs implementation. ElasticSyN has an additional elastic regularization term and SyNRA has an additional rigid transformation within.

A possible measure for the usage or evaluation of image registration is given by a priori defined segmentation masks that mark the pixelwise regions of corresponding organs/segments in all images. Given the segmentations of a reference image \mathcal{R}^s and of a template image \mathcal{T}^s as well as a displacement u , the Dice-score measures the overlap of the deformed segmentation $\mathcal{T}^s[u]$ and \mathcal{R}^s and is given by

$$Dice(\mathcal{T}^s, \mathcal{R}^s, u) = 2 \cdot \frac{|\mathcal{T}^s[u] \cap \mathcal{R}^s|}{|\mathcal{T}^s[u]| + |\mathcal{R}^s|}, \quad (2)$$

where $|\cdot|$ denotes the amount and \cap the intersection of non-zero pixels. To clarify, one can represent the segmentations as sets, consisting of tuples that represent the pixels of the segments. Totally overlapping corresponding segments get the highest possible score of 1, disjoint segments score with 0 (Dice, 1945; Sørensen, 1948).

3 RELATED WORK

At the current state of research, deep learning methods are used for a variety of applications e.g. image recognition, image segmentation, data synthesis, image restoration, natural language processing, image registration etc. In the context of image synthesis, derivations of GANs (Goodfellow et al., 2014) were developed to enable text-to-image synthesis, high-resolution synthesis of human image and even registration of medical images (Reed et al., 2016; Karras et al., 2018; Mahapatra et al., 2018).

In 2017, Zhu and Park et al. introduced the framework CycleGAN, enabling a wide usage of unpaired image-to-image translation tasks (Zhu et al., 2017). Some publications focused on the improvement of the CycleGAN image synthesis in general. By enforcing mutual information (MI) and structural consistency on the synthesis (Ge et al., 2019), adding frequency-supervised architecture between generator and discriminator (Shi et al., 2021), studying the effects of

gradient consistency and training data size (Hiasa et al., 2018a) or using a variety of loss functions to influence the synthesis (Kida et al., 2020), they showed improvements on their individual datasets.

Non-registration use cases for multi-modal image synthesis are widely investigated, especially by using the CycleGAN framework. Wolterink et al. used the CycleGAN to convert brain MR images into synthetic CT images and determined an improvement of the use of unpaired compared to paired training (Wolterink et al., 2017). Others used CycleGAN or similar structures for MR/CT images to investigate the synthesis using paired and unpaired data (Jin et al., 2019), to create missing CT data (Hiasa et al., 2018b) or to improve data segmentation (Jiang et al., 2018; Chartasias et al., 2017). In order to substitute/improve the dose calculations of radiation treatment with CBCT images, some researchers used CycleGAN to synthesize CBCT images to synthetic CT images (Kuckertz et al., 2020; Liang et al., 2019; Gao et al., 2021; Kurz et al., 2019).

For the specific case of image registration with prior image synthesis, there are a few research studies investigating the influence of MR-CT image synthesis on multi-modal image registration. These researches use different datasets and evaluation methods, thereby coming to different results. Wei et al. used CycleGAN synthesis and showed an improvement in image registration performance by evaluating with the rigid and deformable ANTs method (Wei et al., 2019). McKenzie et al. applied the synthesis on images of the head-and-neck area and evaluated the registration performance of a B-spline deformable method, resulting in lower registration errors than without synthesis as a prior (McKenzie et al., 2019). On the other hand, Tanner et al. couldn’t show an overall improvement by synthesizing whole-body MR and CT scans and registering them with deformable registration methods (Tanner et al., 2018). Additionally, Jiahao Lu et al. evaluated the influence of synthesis by CycleGAN and other synthesizing frameworks with the registration performance on the open source datasets ‘Zurich’, ‘Cytological’ and ‘Histological’ and concluded that synthesis is only applicable on easy multi-modal problems (Lu et al., 2021). Apart from using the deep learning synthesis method CycleGAN, some researches utilized synthesis methods from probabilistic frameworks or Patch-wise Random Forests. In these papers, the influence of synthesis was also evaluated using ‘SyN’ as a registration method, among others (Cao et al., 2017; Roy et al., 2014).

Because of the mixed results for the improvement of registration performance with synthetic data, there

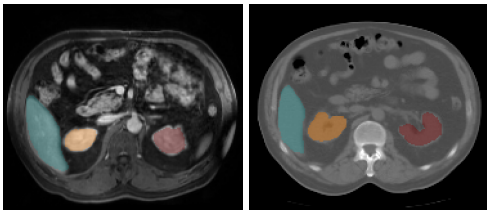


Figure 1: The axial slices of the MR image on the left and the CT image on the right are shown with 3 of their represented segments. [Light blue] as the liver, [orange] as the left kidney and [red] as the right kidney.

is a need to further investigate this application by performing a well-structured analysis of different use cases with different registration methods. We contribute to this analysis of deep learning MR-CT image synthesis on multi-modal image registration by evaluating the performance of four registration methods of the ANTs framework (more precisely ANTsPy). The image synthesis prior to the registration will be performed with a CycleGAN implementation. The MR-CT dataset used in this study consists of abdominal images coming from the Learn2Reg2021-challenge (Dalca et al., 2021).

4 DATASET

In this study, we use the MR and CT abdomen images used in and prepared from the Learn2Reg2021 challenge (Dalca et al., 2021). The 16 paired images from the TCIA dataset (Clark et al., 2013) are split into eight training and eight testing samples. The Learn2Reg organizers additionally have provided manual segmentations for all eight training MR and CT images for the organs liver, spleen, right kidney and left kidney. Furthermore, 40 MR images from the CHAOS dataset (Kavur et al., 2019) as well as 49 CT images from the BCV dataset where additionally provided for training purposes. All images are standardized to the image size $192 \times 160 \times 192$ with a voxel size of $2 \times 2 \times 2$ mm. The challenges of registration in combination of the dataset are given by its multi-modal scans, few/noisy annotations, large deformations and missing correspondences. As an example, Figure 1 shows an MR image and its corresponding CT image with three different colored annotated segments. To further preprocess the data for 2D synthesis, we sliced all volumes into 192×160 axial 2D images and individually removed empty or incomplete slices from the top or bottom of the volumes. Then we replaced the intensities of body surrounding structures to the corresponding background intensity which is -1000 for CT images and 0 for MR images. The CT images were

also clipped into the intensity interval of $[-400, 600]$ to artificially concentrate the relevant intensities. For the follow-up registration process, we prepared the segmentations of the training images to cover up the same volume as the training images after slice reduction. After reduction, there are in total 5,448 MR and 9,189 CT 2D axial image slices available for the synthesis training.

5 EXPERIMENTAL SETUP

The experiment consists of two separate image processing methods executed consecutively. In the image synthesis-stage, we learn the image-to-image translation between unpaired 2D MR and CT images. Afterwards, we use the synthetic CT images (synCT) to investigate the differences in 3D image registration performance between MR/CT and synCT/CT. The source code is provided on github³.

5.1 Image Synthesis

The synthesizing framework used for the training of MR-to-CT synthesis originates from the CycleGAN implementation in PyTorch (Zhu et al., 2017; Isola et al., 2017). In this implementation, the generators correspond to a ResNet structure, consisting of mainly two down- and up-convolution blocks as well as nine residual blocks in the lowest level in between. The discriminators are named as 70PatchGAN and consist of (down-)convolution blocks resulting in a 18×22 output with a 70×70 receptive field. We integrated an additional mutual information loss for the CT-synthesis direction (MI_A) as well as a gradient loss into the training process for further regulation motivated by the research from Ge and Wei et al. and Hiasa et al. (Ge et al., 2019; Hiasa et al., 2018a). The adversarial losses as well as the cycle loss and the identity loss are originally used in the introduced CycleGAN.

The resulting total loss function is then defined as

$$L_{total} = L_{adv_A} + L_{adv_B} + \lambda_{cycle} L_{cycle} + \lambda_{idt} L_{idt} + \lambda_{grad} L_{grad} + \lambda_{MI} L_{MI_A}. \quad (3)$$

While training, the images are loaded in size 175×210 , randomly cropped back to 160×192 and scaled to the intensity range $[-1, 1]$. The generators are updated prior to the discriminators (Zhu et al., 2017).

For the purpose of hyperparameter tuning, three of the eight paired training images described in the

³<https://github.com/nilsFrohwitter/I2I-Synthesis>

dataset Section 4 were extracted and used as validation data. Following the suggestions from the Learn2Reg-team, we chose the images with the numbers 12, 14 and 16 as the validation set. The hyperparameter tuning resulted in the loss weights $\lambda_{cycle} = 5$, $\lambda_{idt} = 0.5$, $\lambda_{grad} = 1$ and $\lambda_{MI} = 0.5$ with 50 epochs of Adam-optimization (Kingma and Ba, 2015) with $\beta = (0.5, 0.999)$ and a constant learning rate of $lr = 0.0002$, followed by 50 epochs with a linear to zero decaying learning rate. With the best hyperparameters found for the training process, we trained eight new models, each one by leaving out one of the eight TCIA a priori defined training images for later testing, performing a leave-one-out evaluation. After training, the resulting eight individual testing images (in their original and synthetic form) are used for the following registration evaluation. The quality assessment of the synthesis is performed by visually comparing the synthetic results with each other and with its corresponding CT and MR images as well as by controlling the synthesis continuity across all axial slices in the 3D images. Thereby, we categorised the images into three quality states: good, medium and bad. In the evaluation of the following image registration, we differentiate the quality of the synthesis and therefore analyze poorly synthesized data separately. In our case, we have badly synthesized test images 06 and 10. Figure 2 shows a synthetic CT image slice of the test images 14 as an example of good synthesis and 10 as a bad one. The synthetic CT image slice of Image 14 shows good intensity adaption while preserving the organ structures properly. On the other hand, the resulting synthetic CT image slice of Image 10 clearly shows major distortions of organ structures after synthesis, which we rate to be an example of bad synthesis. Image 06 also has major distortions after synthesis, resulting especially in a high variation of spine localisation along all image slices.

5.2 Image Registration

Image registration is performed in 3D with registration methods from the ANTsPy framework. We use the methods ‘Rigid’, ‘SyN’, ‘SynRA’ as well as ‘ElasticSyN’ in its predefined states. Because we aim to evaluate the performance gain by using an additional synthesis step, we calculate two registrations (with each method) for the eight images, one using the original MR data and one using the prior synthesized data (synCT). The determined deformations are then applied to the segmentations of their respective MR images.

All registration results are compared by calculating the Dice-score between the deformed segmenta-

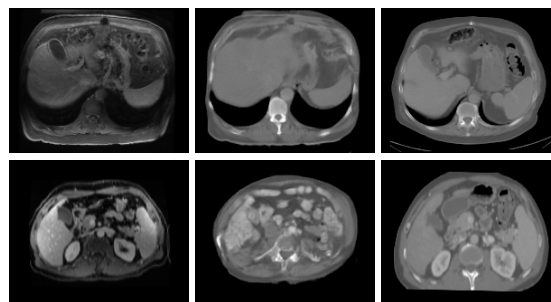


Figure 2: From left to right: MR, synCT, corresponding CT. Note, that the corresponding CT is not properly registered to the MR. The top row shows test image 14 as an example of a good synthesis where intensities are adopted and structures are mainly preserved. The bottom row shows the test image 10 as a bad synthesis example where the synthetic CT is greatly distorted.

tions of the MR images and the segmentations of the CT images. We reduce the influence of randomness in the registration process by performing the whole process of learning, synthesis and registration five times and using the average of all runs.

5.3 Additional Image Meta Data

To further understand and interpret the results of registration in relation to the synthesis quality, we investigate some meta data of the original and synthetic images. We calculate and compare the entropy of the MR and CT images as well as of their synthetic correspondences synCT and synMR. Furthermore, besides visually interpreting, we use the Fréchet Inception Distance (FID) to measure the quality of synthesis in a quantitative way. The FID score compares the mean and standard derivation of the deepest layer of the pretrained Inception v3 model, which highly correlates with human perception of similarity in images (Heusel et al., 2017). The lower the FID score, the better an image represents the target dataset.

6 RESULTS AND DISCUSSION

The results in Table 1 of the four registration methods with and without a prior synthesis step show, that when the synthesis results in realistic synthetic CT images, this synthesis step also improves the average image registration performance. For every ANTsPy method, the average Dice-score of good synthesis cases is higher with the use of the synthetic CT than with the original MR image. The biggest improvement with synthesis in registration performance is achieved for the ‘SyN’ method with 8% Dice-score improvement. The overall best registration method

Table 1: Averaged Dice scores from 5 registration runs of the 6 good synthesized test images between the CT and MR/synthetic CT (sCT) as initial values and after rigid, SyN, SyNRA and ElasticSyN registration. The maximum dice scores per image and the averages over the images are highlighted as bold numbers. The highest Dice-score averaged over the 6 models is acquired for SyNRA with the synthetic CT.

Vol	init	Rigid		SyN		SyNRA		ElasticSyN	
		MR	sCT	MR	sCT	MR	sCT	MR	sCT
02	0.505	0.562	0.559	0.657	0.665	0.648	0.675	0.657	0.659
04	0.095	0.254	0.382	0.497	0.405	0.538	0.526	0.598	0.381
08	0.547	0.786	0.736	0.892	0.853	0.890	0.852	0.892	0.851
12	0.257	0.472	0.538	0.626	0.653	0.620	0.649	0.625	0.654
14	0.196	0.585	0.600	0.121	0.528	0.659	0.730	0.119	0.504
16	0.493	0.693	0.685	0.847	0.826	0.843	0.827	0.856	0.822
<i>avg_{good}</i>	0.349	0.559	0.583	0.606	0.655	0.700	0.710	0.623	0.645

Table 2: Averaged Dice scores from 5 registration runs of the 2 bad synthesizing models between the CT and MR/synthetic CT (sCT) as initial values and after rigid, SyN, SyNRA and ElasticSyN registration. The maximum dice scores per image and the averages over the images are highlighted as bold numbers. The highest Dice-score averaged over the 2 models is acquired for Rigid with the synthetic CT.

Vol	init	Rigid		SyN		SyNRA		ElasticSyN	
		MR	sCT	MR	sCT	MR	sCT	MR	sCT
06	0.465	0.505	0.599	0.401	0.252	0.326	0.272	0.345	0.248
10	0.380	0.502	0.522	0.636	0.321	0.642	0.321	0.637	0.323
<i>avg_{bad}</i>	0.423	0.504	0.561	0.519	0.287	0.484	0.297	0.491	0.286

with prior synthesis is ‘SyNRA’, which achieves a Dice-score of 0.710. As an illustration of the differences in the registration methods used on one test image, the resulting deformed MR segments on top of the CT image with and without synthesis are given in Figure 3 from the test image 14. The different segmentation overlaps on the corresponding CT image are clearly visible, especially for the different registration methods of the MR-CT registration.

Besides, the Dice-scores of the registrations of the badly synthesized images 06 and 10 show a distinct degradation of registration performance in the SyN-methods when using the synthetic CT instead of the original MR image (s. Table 2). Interestingly, Rigid is the only method where the synthesis results in an averaged better Dice-score. For the good synthesized images, it is, on average, the exact other way around. The results clearly show the difference on the registration performance between goodly and badly synthesized images, which leads to the idea of registration improvement by simply further enhancing the synthesizing quality.

Since the synthesis quality plays an important role, we investigated if the change in entropy or the FID score can explain/determine the synthesis quality. Table 3 shows that neither score gives an precise individual explanation to the synthesis quality and registration performance. The FID score of synthetic CT Image 10 (173) is a lot higher than the scores of the other images, considering FID has a range of [88, 173]

Table 3: After the training of the 8 models, the respective resulting synthetic test images are visually assessed to be of good, medium or bad quality. In order to reason this categorization, the entropy (H) as well as the fréchet inception distance (FID) is calculated before and after the MR-to-CT synthesis. The FID score is here defined to be lower if the image better represents the joint dataset of all the 8 corresponding CT images.

image ID	quality (synCT)	H (MR)	H (synCT)	FID (MR)	FID (synCT)
02	good	14.39	5.7	239	88
04	medium	14.59	5.79	219	118
06	bad	14.84	5.72	200	129
08	medium	12.31	5.77	237	123
10	bad	9.93	5.64	226	173
12	good	13.27	5.76	153	122
14	good	13.90	5.76	213	132
16	good	14.18	5.61	186	97

for this data. Since the badly synthesized CT 06 has a FID score of 129 and the goodly synthesized Image 14 has a comparatively high FID score of 132, the reliability of the FID score in terms of synthesis quality and additionally in this research of registration performance is highly questionable, which argues for a necessary manual check of synthesis quality.

7 CONCLUSION

Given the abdominal MR and CT images of the Learn2Reg2021-challenge, we investigated the ef-

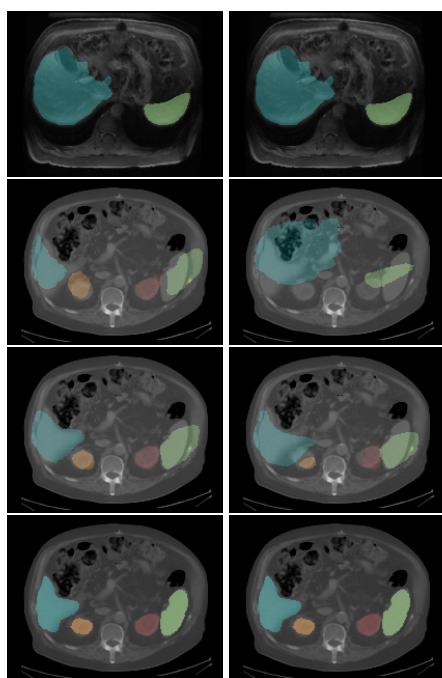


Figure 3: Both columns show the original MR on the top and the original CT on the bottom with its corresponding segmentations (blue: liver, green: spleen, orange: left kidney, red: right kidney). The first column shows the resulting deformed MR-segmentation in the second and third image after registration with ‘SyNRA’, where the second column shows it after ‘ElasticSyN’ registration. The results of the MR-CT registration is visualized in each second image and of the synCT-CT registration in each third image.

effects of prior image synthesis on multi-modal MR-to-CT image registration. Precisely, we trained eight CycleGAN-models individually by leaving out one of the eight TCIA a priori defined training images for later testing and compared the image registration results of four ANTs registration methods (‘Rigid’, ‘SyN’, ‘SyNRA’ and ‘ElasticSyN’) with and without the use of the synthetic CT instead of the original MR image. Additionally, we investigated two metrics for determining synthesis quality. Overall, We show that good synthesizing results lead to an average improvement in all of the four registration methods. Furthermore, the biggest improvement in registration performance is achieved for the ‘SyN’ method with 8% in Dice-score and the overall best registration method with prior synthesis is ‘SyNRA’. These results are an important contribution to the discussion on the usefulness of synthesis for the registration task and show promising positive effects. Additionally, the experiments indicated that further improvements in image synthesis will also benefit the registration task. Future research should aim to make further validation on the synthesis benefits using other datasets and other

multi-modal registration tasks. Also, methods for automatically evaluating the synthesis performance are needed for an automated application of synthesis in registration tasks.

REFERENCES

- Avants, B. B., Tustison, N. J., Song, G., Cook, P. A., Klein, A., and Gee, J. C. (2011). A reproducible evaluation of ants similarity metric performance in brain image registration. *NeuroImage*, 54(3):2033–2044.
- Cao, X., Yang, J., Gao, Y., Guo, Y., Wu, G., and Shen, D. (2017). Dual-core steered non-rigid registration for multi-modal images via bi-directional image synthesis. *Medical image analysis*, 41:18–31.
- Chandarana, H., Wang, H., Tijssen, R., and Das, I. J. (2018). Emerging role of mri in radiation therapy. *Journal of Magnetic Resonance Imaging*, 48(6):1468–1478.
- Chartsias, A., Joyce, T., Dharmakumar, R., and Tsaftaris, S. A. (2017). Adversarial image synthesis for unpaired multi-modal cardiac data. In *International workshop on simulation and synthesis in medical imaging*, pages 3–13. Springer.
- Clark, K., Vendt, B., Smith, K., Freymann, J., Kirby, J., Koppel, P., Moore, S., Phillips, S., Maffitt, D., Pringle, M., et al. (2013). The cancer imaging archive (tcia): maintaining and operating a public information repository. *Journal of digital imaging*, 26(6):1045–1057.
- Dalca, A., Hering, A., Hansen, L., and Heinrich, M. P. (2021). Grand challang: Learn2reg2021. Accessed: 2022-07-20.
- Dice, L. R. (1945). Measures of the amount of ecologic association between species. *Ecology*, 26(3):297–302.
- Gao, L., Xie, K., Wu, X., Lu, Z., Li, C., Sun, J., Lin, T., Sui, J., and Ni, X. (2021). Generating synthetic ct from low-dose cone-beam ct by using generative adversarial networks for adaptive radiotherapy. *Radiation Oncology*, 16(1):1–16.
- Ge, Y., Wei, D., Xue, Z., Wang, Q., Zhou, X., Zhan, Y., and Liao, S. (2019). Unpaired mr to ct synthesis with explicit structural constrained adversarial learning. In *2019 IEEE 16th International Symposium on Biomedical Imaging (ISBI 2019)*, pages 1096–1099.
- Goodfellow, I., Pouget-Abadie, J., Mirza, M., Xu, B., Warde-Farley, D., Ozair, S., Courville, A., and Bengio, Y. (2014). Generative adversarial nets. pages 2672–2680.
- Heusel, M., Ramsauer, H., Unterthiner, T., Nessler, B., and Hochreiter, S. (2017). Gans trained by a two time-scale update rule converge to a local nash equilibrium. In Guyon, I., Luxburg, U. V., Bengio, S., Wallach, H., Fergus, R., Vishwanathan, S., and Garnett, R., editors, *Advances in Neural Information Processing Systems*, volume 30. Curran Associates, Inc.
- Hiasa, Y., Otake, Y., Takao, M., Matsuoka, T., Takashima, K., Carass, A., Prince, J. L., Sugano, N., and Sato, Y. (2018a). Cross-modality image synthesis from unpaired data using cyclegan. In *International workshop*

- on simulation and synthesis in medical imaging, pages 31–41. Springer.
- Hiasa, Y., Otake, Y., Takao, M., Matsuoka, T., Takashima, K., Carass, A., Prince, J. L., Sugano, N., and Sato, Y. (2018b). Cross-modality image synthesis from unpaired data using cyclegan. In Gooya, A., Goksel, O., Oguz, I., and Burgos, N., editors, *Simulation and Synthesis in Medical Imaging*, pages 31–41, Cham. Springer International Publishing.
- Isola, P., Zhu, J.-Y., Zhou, T., and Efros, A. A. (2017). Image-to-image translation with conditional adversarial networks. In *Computer Vision and Pattern Recognition (CVPR), 2017 IEEE Conference on*.
- Jiang, J., Hu, Y.-C., Tyagi, N., Zhang, P., Rimner, A., Mageras, G. S., Deasy, J. O., and Veeraraghavan, H. (2018). Tumor-aware, adversarial domain adaptation from ct to mri for lung cancer segmentation. In *International conference on medical image computing and computer-assisted intervention*, pages 777–785. Springer.
- Jin, C.-B., Kim, H., Liu, M., Jung, W., Joo, S., Park, E., Ahn, Y. S., Han, I. H., Lee, J. I., and Cui, X. (2019). Deep ct to mr synthesis using paired and unpaired data. *Sensors*, 19(10):2361.
- Karras, T., Laine, S., and Aila, T. (2018). A style-based generator architecture for generative adversarial networks. *CoRR*, abs/1812.04948.
- Kavur, A. E., Selver, M. A., Dicle, O., Barış, M., and Gezer, N. S. (2019). CHAOS - Combined (CT-MR) Healthy Abdominal Organ Segmentation Challenge Data.
- Kida, S., Kaji, S., Nawa, K., Imae, T., Nakamoto, T., Ozaki, S., Ohta, T., Nozawa, Y., and Nakagawa, K. (2020). Visual enhancement of cone-beam ct by use of cyclegan. *Medical physics*, 47(3):998–1010.
- Kingma, D. P. and Ba, J. (2015). Adam: A method for stochastic optimization. In Bengio, Y. and LeCun, Y., editors, *3rd International Conference on Learning Representations, ICLR 2015, San Diego, CA, USA, May 7-9, 2015, Conference Track Proceedings*.
- Kuckertz, S., Papenberg, N., Honegger, J., Morgas, T., Haas, B., and Heldmann, S. (2020). Learning deformable image registration with structure guidance constraints for adaptive radiotherapy. In Špiclin, Ž., McClelland, J., Kybic, J., and Goksel, O., editors, *Biomedical Image Registration*, pages 44–53, Cham. Springer International Publishing.
- Kurz, C., Maspero, M., Savenije, M. H., Landry, G., Kamp, F., Pinto, M., Li, M., Parodi, K., Belka, C., and Van den Berg, C. A. (2019). Cbct correction using a cycle-consistent generative adversarial network and unpaired training to enable photon and proton dose calculation. *Physics in Medicine & Biology*, 64(22):225004.
- LeCun, Y., Bengio, Y., and Hinton, G. (2015). Deep learning. *nature*, 521(7553):436–444.
- Liang, X., Chen, L., Nguyen, D., Zhou, Z., Gu, X., Yang, M., Wang, J., and Jiang, S. (2019). Generating synthesized computed tomography (ct) from cone-beam computed tomography (cbct) using cyclegan for adaptive radiation therapy. *Physics in Medicine & Biology*, 64(12):125002.
- Lu, J., Öfverstedt, J., Lindblad, J., and Sladoje, N. (2021). Is image-to-image translation the panacea for multimodal image registration? a comparative study. *arXiv preprint arXiv:2103.16262*.
- Mahapatra, D., Antony, B., Sedai, S., and Garnavi, R. (2018). Deformable medical image registration using generative adversarial networks. In *2018 IEEE 15th International Symposium on Biomedical Imaging (ISBI 2018)*, pages 1449–1453. IEEE.
- McKenzie, E., Santhanam, A., Ruan, D., O’Connor, D., Cao, M., and Sheng, K. (2019). Multimodality image registration in the head-and-neck using a deep learning derived synthetic ct as a bridge. *Medical Physics*, 47.
- Modersitzki, J. (2009). *Fair: Flexible Algorithms for Image Registration*. Society for Industrial and Applied Mathematics, USA.
- Qi, X. S. (2017). *Image-Guided Radiation Therapy*, pages 131–173. Springer International Publishing, Cham.
- Reed, S., Akata, Z., Yan, X., Logeswaran, L., Schiele, B., and Lee, H. (2016). Generative adversarial text to image synthesis. In Balcan, M. F. and Weinberger, K. Q., editors, *Proceedings of The 33rd International Conference on Machine Learning Research*, volume 48 of *Proceedings of Machine Learning Research*, pages 1060–1069, New York, New York, USA. PMLR.
- Roy, S., Carass, A., Jog, A., Prince, J., and Lee, J. (2014). Mr to ct registration of brains using image synthesis. *Proceedings of SPIE*, 9034.
- Saiti, E. and Theoharis, T. (2020). An application independent review of multimodal 3d registration methods. *Computers & Graphics*, 91:153–178.
- Shi, Z., Mettes, P., Zheng, G., and Snoek, C. (2021). Frequency-supervised mr-to-ct image synthesis.
- Sørensen, T. J. (1948). *A method of establishing groups of equal amplitude in plant sociology based on similarity of species content and its application to analyses of the vegetation on Danish commons*, volume 5.
- Tanner, C., Ozdemir, F., Profanter, R., Vishnevsky, V., Konukoglu, E., and Goksel, O. (2018). Generative adversarial networks for mr-ct deformable image registration.
- Wei, D., Ahmad, S., Huo, J., Peng, W., Ge, Y., Xue, Z., Yap, P.-T., Li, W., Shen, D., and Wang, Q. (2019). Synthesis and inpainting-based mr-ct registration for image-guided thermal ablation of liver tumors. In *International Conference on Medical Image Computing and Computer-Assisted Intervention*, pages 512–520. Springer.
- Wolterink, J. M., Dinkla, A. M., Savenije, M. H. F., Seevinck, P. R., van den Berg, C. A. T., and Isgum, I. (2017). Deep MR to CT synthesis using unpaired data. *CoRR*, abs/1708.01155.
- Yi, Z., Zhang, H., Tan, P., and Gong, M. (2017). Dualgan: Unsupervised dual learning for image-to-image translation.
- Zhu, J.-Y., Park, T., Isola, P., and Efros, A. A. (2017). Unpaired image-to-image translation using cycle-consistent adversarial networks. In *Computer Vision (ICCV), 2017 IEEE International Conference on*.